Atmos. Chem. Phys. Discuss., 9, 3401–3434, 2009
www.atmos-chem-phys-discuss.net/9/3401/2009/

Atmospheric Chemistry and Physics Discussions

This discussion paper is/has been under review for the journal *Atmospheric Chemistry and Physics (ACP)*. Please refer to the corresponding final paper in *ACP* if available.

Do gravity waves significantly impact PSC occurrence in the Antarctic?

A. J. McDonald, S. E. George, and R. M. Woollands

Department of Physics and Astronomy, University of Canterbury, Private Bag 4800, Christchurch, New Zealand

Received: 11 December 2008 – Accepted: 8 January 2009 – Published: 3 February 2009

Correspondence to: A. J. McDonald (adrian.mcdonald@canterbury.ac.nz)

Published by Copernicus Publications on behalf of the European Geosciences Union.

Abstract

This study uses a combination of POAM III aerosol extinction measurements and CHAMP GPS/RO temperature measurements to examine the role of atmospheric gravity waves in Polar Stratospheric Cloud (PSC) formation in the Antarctic. POAM III aerosol extinction observations are used to identify Type I Polar Stratospheric Clouds using an unsupervised clustering algorithm. The seasonal and spatial distribution of PSCs observed by POAM III is examined to determine whether there is a bias towards regions of high wave activity early in the Antarctic winter which may enhance PSC formation.

Examination of the probability of temperatures below the Type Ia formation temperature threshold based on UKMO analyses displays a good correspondence to the PSC occurrence derived from POAM III extinction data in general. However, in June the POAM III observations of PSC are more abundant than expected from temperature thresholds. In addition the PSC occurrence based on temperature thresholds in September and October is often significantly higher than the PSC occurrence observed by POAM III, this observation probably being due to dehydration and denitrification. Use of high resolution temperatures from CHAMP GPS/RO observations provide a slightly improved relationship to the POAM III derived values. Analysis of the CHAMP temperature observations indicates that temperature perturbations associated with gravity waves may explain the enhanced PSC incidence observed in June compared to the UKMO analyses. Comparison of the UKMO analyses temperatures relative to corresponding CHAMP observations also suggests a small warm bias in the UKMO analyses during June. Examination of the longitudinal structure PSC occurrence in June 2005 also shows that regions of enhancement are associated with data near the Antarctic peninsula a known Mountain wave “hotspot”. The impact of temperature perturbations causing enhanced temperature threshold crossings is shown to be particularly important early in the Antarctic winter while later in the season temperature perturbations associated with gravity waves could contribute to about 15% of the PSC

observed, a value which corresponds well to several previous studies.

1 Introduction

The role of PSCs in polar ozone depletion was first identified over twenty years ago (Solomon et al., 1986). Heterogeneous chemical reactions on PSC particles are the central process in chlorine activation and consequent ozone depletion. In addition to the activation of chlorine from reservoirs of HCl and $ClONO_2$, PSCs can also remove NO_y (i.e. the total odd nitrogen) from the lower stratosphere by incorporation of HNO_3 from the gas phase and subsequent sedimentation. This denitrification leads to a slower conversion of active chlorine back to the reservoir species $ClONO_2$.

In contrast to the Northern Hemisphere, very low stratospheric temperatures in the Antarctic winter generally lead to an abundance of PSCs in the lower stratosphere (Poole and Pitts, 1994). Three categories of PSCs are generally recognized: type Ia, composed of solid phase nitric acid trihydrate (NAT); type Ib, composed of supercooled ternary solution (STS, a liquid mixture of H_2O, HNO_3, and H_2SO_4); and type II, composed primarily of ice (see Lowe and MacKenzie, 2008, and references therein). All three types of clouds are present during the Antarctic winter. A number of other potential PSC categories have also been proposed, the most relevant to this study is PSC Ia enhanced (Tsias et al., 1999). The present study examines the potential contribution of internal gravity waves to PSC formation in the Antarctic stratosphere. In the Arctic the temperature perturbations associated with internal gravity waves, particularly Mountain waves, have been shown to be responsible for the formation of a significant proportion of PSCs (Carslaw et al., 1998; Hopfner et al., 2001). The observed seasonally driven relationship between Antarctic PSC formation and low temperatures has led to less focus on wave induced PSC formation processes in the Antarctic. However, recent studies have indicated that the temperature perturbations related to these waves have a more significant affect on Antarctic PSC occurrence than previously thought (Shibata et al., 2003; Hopfner et al., 2006; Innis and Klekociuk, 2006). Such effects may be particularly significant in early winter. Recent analysis using data from CALIPSO has also mentioned the potential importance of gravity waves on PSC formation (Pitts et al., 2007; Noel et al., 2008). However, it is also worthy of note that enhanced PSC formation may be associated with synoptic-scale motions (Teitelbaum et al., 2001; Wang et al., 2008).

Shibata et al. (2003) observed PSCs composed of ice particles, over the Syowa Antarctic station, when the stratospheric temperature dropped below the ice condensation point (T_{ICE}). They showed a case in which the Type II PSC formation was only possible because of a low-temperature perturbation associated with a nonorographic gravity wave. They suggested that inertia gravity waves can play a significant role in the formation of solid PSC particles, since the existence of these waves is not limited by the geographical location of high mountains.

Analysis by Hopfner et al. (2006) has also identified a potentially significant role of Mountain waves in the formation of PSC in the Antarctic. Hopfner et al. (2006) described spaceborne infrared measurements of a vortex-wide area of NAT PSC around Antarctica using the MIPAS instrument. Concurrent mesoscale microphysical simulations for the period 10–12 June 2005 indicate the observations are likely to be associated with heterogeneous nucleation on ice in the cooling phases of large-amplitude stratospheric mountain waves over the Antarctic Peninsula. The process operating here is the same Mountain wave NAT formation model originally proposed by Carslaw et al. (1998) for the Arctic winter stratosphere. Note that a large number of studies have shown that the Antarctic peninsula can be considered to be a "hotspot" for gravity wave activity (Wu and Jiang, 2002; Baumgaertner and McDonald, 2007) and therefore might be a potential region of enhanced PSC occurrence.

Another study by Innis and Klekociuk (2006) used lidar observations, at the Davis Antarctic station, to estimate the relative influence of planetary and gravity waves on PSC occurrence. They concluded that during the "PSC season" the background temperature was close enough to the NAT formation temperature (T_{NAT}), derived in Hanson and Mauersberger (1988), for gravity wave perturbations to influence PSC formation approximately 15 percent of the time. Interestingly, this value is similar to the findings of Felton et al. (2007) who concluded type Ia enhanced PSCs makes up about 11% of the clouds observed during the SAGE III Ozone Loss and Validation Experiment (SOLVE) campaign in the Northern Hemisphere. The work by Innis and Klekociuk (2006) also indicated that there is a clear relationship between planetary wave temperature perturbations and PSC occurrence over Davis in winter.

Work has shown that homogeneous NAT nucleation does not occur directly on temperatures crossing the Nitric Acid Trihydrate (NAT) temperature threshold, T_{NAT} (Hanson and Mauersberger, 1988). Rather, average temperatures need to be below the T_{NAT} threshold for a period greater than a few days for nucleation to occur (Peter, 1997). Carslaw et al. (1994) discusses NAT formation and indicates that NAT may form by heterogeneous nucleation on pre-existing ice particles, requiring temperatures below T_{ICE} at some point. Note that the T_{ICE} point occurs at approximately 7 K below T_{NAT} and STS droplets form at temperatures approximately 3.5 K cooler than T_{NAT} (Carslaw et al., 1994). However, recent work has identified a need for NAT nucleation mechanisms which are independent of the existence of ice particles, only requiring temperatures below the existence temperature for NAT which is significantly easier to meet than the demand for pre-existing ice particles. For example, Voigt et al. (2005) detailed measurements where the conditions of particle formation are well enough constrained to conclude that a PSC is observed in air parcels that spent less than a day (approximately 18 h) at temperatures no lower than 3 K below T_{NAT}. An exposure to temperatures below T_{ICE} can be excluded from their study.

In addition, a study detailed in Hitchman et al. (2003) highlights the potential importance of nonorographic gravity waves on PSC formation in the Arctic. Their study also suggests that a formation mechanism for Type Ia PSC must exist without the requirement for temperatures significantly below T_{NAT}. Work by Svendsen et al. (2005) compared model runs with observations and concludes that the correspondence between the observations and the model output is best when NAT nucleation above T_{ICE} is allowed. In the case of the local scale model runs detailed in Svendsen et al. (2005)

the amount of PSC Ia is only slightly affected by the inclusion of Mountain wave effects, whereas Mountain waves have a noticeable impact on the amount of PSC type II. However, the PSC Ia distribution and quantity is relatively poorly estimated. Thus, in this study we attempt to examine the impact of localized temperature variations which produce temperature threshold crossings over the T_{NAT}, T_{STS} and T_{ICE} thresholds.

Work by Pagan et al. (2004) also supported the view that Type Ia PSC formation can occur without the presence of ice particles. Their study concluded that Type Ia PSCs can nucleate in relatively warm synoptic-scale temperature fields and are not limited to forming in, or downwind of, regions of strong mountain-wave activity with sufficient cooling to produce ice nuclei. In addition, Irie et al. (2004) used ILAS trace gas and aerosol extinction measurements, AVHRR stratospheric ice cloud measurements, and a microphysical box model to investigate processes leading to denitrification in the Arctic vortex in February 1997. Their analysis suggest that sedimentation of NAD or NAT particles formed through NAD freezing on aerosol surfaces can cause significant denitrification in the Arctic vortex. Their analysis combined with the results in Pagan et al. (2004) seem to confirm that ice particle surfaces are not a prerequisite for the formation of nitric acid hydrate PSCs. Review of these and other studies detailed in the World Meteorological Organization (2007) report indicates increasing evidence that processes occur above the ice frost point. However, the report indicates that whether these processes are applicable in the Antarctic requires investigation.

Previous work by Wang and Lin (2007) compared GPS/RO derived temperature soundings in the Antarctic winter stratosphere with corresponding radiosonde data over the South Pole and Neumayer stations. The GPS/RO soundings, which include measurements at higher altitudes than is possible for the balloon flights, show that the coldest atmospheric temperatures, below the T_{NAT} threshold (Hanson and Mauersberger, 1988), generally occur in an 18 km-thick vertical layer between 10 and 28 km above sea level during the southern hemisphere winter season. Thus, high quality measurements of vertical temperature structure over the Antarctic region are important inputs for models that predict polar stratospheric clouds occurence and stratospheric ozone depletion (Huck et al., 2005). For this reason, previous studies have focused on identifying the frequency of crossing different temperature thresholds associated with PSC formation (Pawson et al., 1999; Wang and Lin, 2007; Parrondo et al., 2007). It should be noted that continuous observations of temperature profiles over the Antarctic region have been very limited; moreover, inspection of the reanalysis data over the Antarctic region shows a cold bias and an unrealistic vertical structure (Parrondo et al., 2007).

Parrondo et al. (2007) compared temperatures from radiosondes launched at Belgrano and other Antarctic stations in support of the QUOBI campaign with the ECMWF and NCEP operational models for the 2003 Antarctic winter. Their results show good agreement between radiosondes and NCEP and a bias in ECMWF fields which is height-dependent. The ECMWF model bias results in an overestimate of the potential PSC presence, and hence the surface available for heterogeneous reactions. This effect is particularly significant at the 375 and 510 K isentropic levels where ozone is not completely depleted. Their study argues that small temperature changes at these levels could have significant impacts on the computation of the depletion in the integrated ozone column. At the 525 K isentropic level the overestimate for the whole season is 8% for PSC type I and 29% for PSC type II.

To our knowledge a quantification of the importance of gravity waves on PSC formation across the entire Antarctic has not been performed. This study examines the relationship between PSC occurrence observed using POAM III observations and the occurrence expected based on UKMO analyses and CHAMP radio occultation measurements. The addition of high vertical resolution CHAMP temperature observations provides the possibility of identifying periods and spatial regions where PSC formation associated with gravity wave induced temperature perturbations may occur. Comparison of the observations from UKMO analyses and CHAMP observations also allows the sensitivity of PSC occurrence to temperature biases in UKMO analyses to be examined. In order to examine the importance of temperature and the impact of gravity wave temperature perturbations we determine the probability that a region is below various threshold temperatures relative to the frequency of PSC observations made with

POAM III. This method has previously been used by many authors, including Poole and Pitts (1994) and Saitoh et al. (2006).

As indicated previously, this study aims to use a mixture of POAM III, CHAMP RO observations and UKMO analyses to identify whether the influence of gravity wave temperature perturbations can be observed and also how important this is in overall PSC formation. Section 2 briefly describes the POAM III and CHAMP RO observations and also details a new unsupervised clustering algorithm which is applied to POAM III extinction measurements to identify PSC. Comparisons of the observed probability of PSC occurrence relative to those based on the occurrence of temperatures below the T_{NAT}, T_{STS} and T_{ICE} thresholds derived from UKMO analyses and CHAMP RO data are detailed in Sect. 3 and the interpretation of these results is discussed in Sect. 4.

2 Dataset and methodology

The POAM III instrument made observations of the upper troposphere and stratosphere between its launch on the Satellite Pour l'Observation de la Terre (SPOT) 4 satellite in March 1998 and the end of 2005. POAM measures water vapor, aerosol extinction, ozone, and nitrogen dioxide using the solar occultation limb sounding technique (Lucke et al., 1999). The high inclination of the SPOT 4 satellite allows occultations to be performed in both the northern and southern polar regions. It should be noted that the POAM III sampling volume is about 200 km long, 30 km wide, and 1 km thick and thus this data set will not capture very small-scale features. Research completed by POAM III has focused on examinations of the spatial and temporal variability of stratospheric ozone, aerosols, polar stratospheric clouds, and polar mesospheric clouds.

In this work, Type Ia and Ib PSC (or alternatively NAT or STS PSC) occurrence is derived from POAM III extinction measurements at 1.018 μm and the ratio of the 1.018 to the 0.603 μm extinction channels using a k-means unsupervised clustering algorithm. Jakob and Tselioudis (2003) have previously utilized a simple clustering algorithm for cloud regime identification in the Tropical Western Pacific region and recent work by Felton et al. (2007) has applied a clustering algorithm to lidar observations of PSC. We use a similar method to that indicated in Jakob and Tselioudis (2003) to separate different types of PSC. Our algorithm identifies both Type Ia and Ib aerosols using the methodology described in Strawa et al. (2002) except that the separation is based on an unsupervised clustering algorithm. Note in this study we do not differentiate between Type Ia and Ib PSC and only examine the occurrence of Type I PSCs. The separation into different types will be left to a future study. It should be noted that this method provides similar PSC identification ability to algorithms described by Fromm et al. (2003).

The statistical method of cluster analysis is used to separate background aerosol extinctions from those associated with PSCs. As its name suggests, cluster analysis searches for possible "clusters" in a data set by evaluating some measure of distance between individual data points (in this study we use Euclidean distance in extinction ratio/extinction space to separate PSC and none PSC observations and then an angular measure to separate PSC Type Ia and Ib PSCs). It should be noted that to ensure that neither the extinction at 1.018 μm or the ratio of 1.018 to the 0.603 μm extinction channels dominate in the clustering procedure the values are normalized. Note that in this case a "data point" is an individual set of measurements of aerosol extinction from POAM III at a specific altitude and geographical location. This study uses a k-means clustering algorithm. This algorithm iteratively searches for a predefined number (k) of clusters, two in this case, using the following scheme:

1. k elements of the data set of size N are selected at random as distinct cluster members;
2. each of the remaining N-k elements are assigned to the cluster with the nearest centroid (based on Euclidean distance in extinction ratio/extinction) whereby after each assignment the centroid of the cluster is recalculated; and
3. after all elements have been assigned the centroids found in step 2 are used as

new seed points and the algorithm is iterated.

Normally fewer than ten iterations are sufficient for the convergence of the algorithm. A second almost identical algorithm then separates the resultant PSC measurements into Type Ia and Ib using a similar procedure, but using a different separation metric. Note that the random selection of data points indicated in the algorithm does not work on observations from the Arctic because of the small number of observations which include PSC. This is because it becomes difficult to identify physically meaningful clusters initially at random. Thus, some apriori knowledge to select likely PSCs would be required. For example, a methodology similar to Fromm et al. (2003) could be used.

It should be noted at this point that other studies (Fromm et al., 1997, 2003) have indicated that the high extinctions associated with Type II PSC can cause the termination or commencement of occultation events at anomalously high altitudes. This is caused by the PSC having large opacity and/or size preventing POAM III measuring lower. Thus, the extinctions measurements are useful for identifying Type I PSC only.

This study also employs data from the radio occultation (RO) experiment onboard the CHAMP satellite. In this experiment GPS radio signal bending due to atmospheric refractivity is measured to determine profiles of atmospheric parameters. The data was processed and provided by the GeoForschungsZentrum (GFZ) Potsdam. Version 005 was used for this study. Specific information on the processing method used is deatiled in Wickert et al. (2004). The CHAMP satellite has an inclination of 87° and therefore the data distribution over the globe is nearly uniform. Inversion of bending angle information allows the instrument to produce approximately 150-200 profiles of dry temperature each day. From Fresnel diffraction theory it can be shown that the profiles have a true vertical resolution of approximately 1.4 km in the stratosphere. However, the data is over-sampled and provided by the GFZ at a vertical resolution of 200 m. The horizontal resolution of an occultation is 200–400 km along the line of sight (LOS) and on the order of 1–3 km across the LOS. A large number of studies have described the quality of these temperature measurements (McDonald and Hertzog, 2008, and references therein).

Temperatures obtained from CHAMP observations and UKMO analyses are used to determine the frequency of temperatures below various temperature thresholds in this study. The NAT PSC formation temperature has been shown to be dependent on the nitric acid and water vapour concentration (Hanson and Mauersberger, 1988). The NAT formation temperature, T_{NAT}, at 18 km as derived using the formulation of Hanson and Mauersberger (1988) which is a function of nitric acid and water vapour concentrations is shown in Fig. 1, the ranges selected are typical of concentrations in the polar stratosphere. Figure 1 clearly shows that T_{NAT} varies much more as a function of water vapour than nitric acid mixing ratios for the ranges typical of the Antarctic stratosphere chosen in this diagram. The selection of these values is based on nitric acid concentrations identified in Santee et al. (2007) and typical water vapour concentrations at this altitude measured by the POAM III instrument (see Fig. 2). The probability of crossing the NAT formation temperature threshold is thus determined by comparing UKMO and CHAMP temperature observations at a specific altitude with the T_{NAT} threshold derived using the formulation of Hanson and Mauersberger (1988) for that altitude. The H_2O variation used is taken from the POAM III observations and a constant nitric acid mixing ratio of 10 ppbv is assumed unless indicated otherwise in the text. To determine the STS formation temperature we use the well-known approximation that the T_{STS} threshold occurs at 3.5 K below the value of T_{NAT} (Carslaw et al., 1994). In a similar manner the ice formation temperature is approximated by using a value 7 K below the value of T_{NAT}.

A time-altitude contour plot of the water vapour mixing ratio for the period January 2002 to December 2005, used in the temperature threshold calculations displayed in Fig. 4, is shown in Fig. 2. Examination of the seasonal variation of water vapour mixing ratio displays a consistent irreversible dehydration potentially associated with the sedimentation of ice PSC at altitudes between 12 and 20 km between August and September each year. At higher altitudes, above 20 km, higher water vapour mixing ratios are observed which are likely to be associated with diabatic descent (Nedoluha et al., 2003).

Uncertainties on the probabilities displayed later in this study are derived assuming a binomial distribution in a similar manner to that utilised in Alfred et al. (2007). The standard deviation of a binomial distribution, σ, can be written as:

$$\sigma = \frac{\sqrt{Np(1-p)}}{N} \quad (1)$$

where N is the number of observations and p is the probability.

3 Results

Figure 3 displays a time-altitude contour plot of the median UKMO analyses temperature interpolated to the positions of POAM III observations overlaid are two contours associated with PSC occurrence probabilities at the 25 and 75% levels, respectively, determined from POAM III extinction measurements in 2000. To ensure a large enough statistical sample, probabilities are calculated using a sliding 10-day window. Examination of Fig. 3 suggests a strong correspondence between temperature and PSC occurrence, this relationship being particularly clear in June and July.

Figure 4 displays the probability of temperatures below T_{NAT} based on UKMO analyses (red line), the STS PSC formation temperature (green line), T_{STS}, and the ice nucleation temperature (blue line), T_{ICE}, against time of year. Figure 4 also displays the probability of PSC detection based on the k-means detection algorithm applied to POAM III observations (black line). It should be noted that the values in Fig. 4 are the probabilities of PSC occurrence derived over a 10 day interval at 18km. This methodology should provide accurate values of both PSC occurrence and temperature threshold crossings, but the daily values plotted will not be independent. Figure 4 also displays the uncertainties, represented by one standard deviation from the mean, on each derived probability on the fifteenth day of each month for reference purposes. Note that problems with the POAM III instrument produce data gaps in the 2004 observations displayed in Fig. 4. Examination of Fig. 4 shows the expected increase in PSC incidence from June to September and a general reduction in occurrence after this date associated with changes in temperature, nitric acid and water vapour concentrations. However, comparison of the PSC occurrence predicted from temperature threshold crossings and those derived from POAM III extinction data do not correspond within the defined uncertainties in several regions.

Averaged over the entire period identified the T_{NAT} temperature threshold derived from UKMO analyses predicts more PSC than observed by POAM III. This is to be expected because Type Ia PSC formation requires average temperatures below the T_{NAT} threshold for a period. The exact temperature value required varies dependent on whether NAT only forms by heterogeneous nucleation on pre-existing ice particles, requiring temperatures below T_{ICE} (Carslaw et al., 1994), or NAT nucleation mechanisms independent of the existence of ice particles exist (Hitchman et al., 2003; Pagan et al., 2004; Svendsen et al., 2005). The POAM III observations predict between 60 and 70% of the occurrence identified by the T_{NAT} temperature threshold in all the years except 2002 where only 44% of the PSC predicted by the T_{NAT} threshold is observed. Comparison of the PSC occurrence observed by POAM III and identified by the T_{STS} temperature threshold displays a better correspondence, but this threshold still overestimates the quantity of PSC. In this case, the POAM III observations predict between 78 to 99% of the PSC frequency identified by the T_{STS} threshold apart from in 2002 and 2003 where only 60% of the predicted PSC is observed by POAM III. It should be noted that this result concurs with recent CALIPSO observations detailed in Pitts et al. (2007) which suggest that the T_{STS} temperature threshold may be a better measure of PSC existence than the T_{NAT} threshold. Inspection of the frequency of PSC occurrence identified by the T_{ICE} threshold derived from UKMO analyses and the POAM III frequency suggests the T_{ICE} occurrence generally significantly underestimates the quantity of PSC observed by POAM III.

Close examination of Fig. 4 indicates that, during certain years (specifically 2002 and 2005), the observed quantity of PSC in June is greater than that predicted from T_{NAT}

and T_{STS} temperature thresholds alone. Analysis (not shown here) indicates that this pattern does not change significantly even if the nitric acid mixing ratio is increased to 15 ppbv; this change would make the temperature threshold warmer and thus easier to cross. It is also noticeable that at all other periods of the year the probability of PSC occurrence from POAM III measurements is smaller than the expected value based on the proportion of observations below the T_{NAT} threshold. The probability of PSC occurrence based on the T_{ICE} temperature threshold does not exceed the probability of occurrence based on POAM III observations in any of the eight observational years until after early August. Comparison of PSC occurrence based on POAM III observations with the quantity of UKMO analyses data below the T_{STS} threshold shows a greater, but not perfect, correspondence which is generally best between the start of July and the start of September. It should be noted that the temperature thresholds determined account for variations in the water vapour mixing ratio based on POAM III observations, but that the nitric acid is held constant at 10 ppbv. Previous studies suggest that the difference between the occurrence probability based on POAM III observations and those based on temperature thresholds later in the season is due to denitrification and dehydration (Nedoluha et al., 2003; Alfred et al., 2007). Note also that while not shown here Type Ia PSCs are identified almost exclusively by the unsupervised clustering algorithm in June and early July in all years.

As previously indicated NAT particles probably normally form at temperatures several degrees colder than T_{NAT} (Tabazadeh et al., 2001) or at even lower temperatures (Carslaw et al., 1998). Therefore, a high probability of PSC formation would not be expected in June even if the probability of temperatures crossing the T_{NAT} temperature threshold was relatively large unless a mechanism for Type Ia cloud formation that requires temperatures only below T_{NAT} exists. This study examines whether the enhanced PSC occurrence observed can be explained by gravity wave motions. It should be noted that previous work by Saitoh et al. (2006) has identified a similar enhanced PSC occurrence in June 2003 compared to that identified by temperature thresholds using ILAS-II data.

ACPD

9, 3401–3434, 2009

This study now examines the potential of gravity waves to cause more temperature threshold crossings than expected from the mean represented by UKMO analyses and in particular attempts to identify whether the enhanced PSC frequency in June may be associated with temperature variations that are not resolved in the UKMO analyses. To examine this we use high vertical resolution measurements made by the CHAMP/GPS RO instrument available between 2002 and 2005. It should be noted that the CHAMP observations are not dense enough to directly identify the presence of gravity waves at POAM III measurement locations and thus we are limited to examining the enhanced temperature threshold crossing frequency produced by gravity waves in a statistical sense. The latitudinal variation of the POAM III observations has been accounted for in this statistical analysis, this variation being displayed in the upper panel of Fig. 8. We begin by displaying a single CHAMP temperature profile observed on 2nd June 2006 (see Fig. 5). Figure 5 also displays the mean temperature derived by applying a 4th order polynomial fit to the CHAMP observations (red line) and the T_{NAT} (blue line) and T_{ICE} (blue dashed line) temperature thresholds. This temperature profile displays a clear wave-like structure. The temperature perturbations associated with the gravity wave (the difference between the red and green lines) allow the T_{NAT} threshold to be crossed at around 17 km and between approximately 20 and 21 km, while the mean temperature profile does not cross the T_{NAT} threshold. It should also be noted that the temperature perturbations, typically ±2 K, do not cross the T_{ICE} threshold. This is typical for this period of the year, but periods where the temperature perturbations associated with gravity waves allow a crossing of the T_{STS} or the T_{ICE} threshold do occur later in the season. It should be noted that the magnitude of the temperature perturbations observed corresponds well to those identified in Innis and Klekociuk (2006).

The upper panel in Fig. 6 displays the probability of the CHAMP temperature measurement being below T_{NAT} (green stars), the probability of the UKMO analyses temperature being below T_{NAT} for various values of HNO_3 mixing ratio (red lines) and the occurrence of PSC based on POAM III observations during 2005. The values in Fig. 6 represent the probabilities of PSC occurrence over the altitude range 12 to 24 km over

10 day intervals and thus each value represents a calculation over up to 1820 measurement. This value varies based on the quality of the observations and will vary because of the high extinctions associated with Type II PSC which can cause the termination or commencement of occultation events at anomalously high altitudes. Figure 6 also displays the uncertainties, represented by three standard deviations from the mean, on each derived probability on the fifteenth day of each month for reference purposes. It should be noted that the uncertainties are such that the one standard deviation points around the mean are so small they are comparable with the width of the line. The lower panel in Fig. 6 shows the difference between that expected from UKMO analyses and the POAM III observations (blue lines) and the enhanced PSC threshold crossings associated with gravity waves based on CHAMP observations (green stars). Examination shows that the monthly values for CHAMP shown in the top panel of Fig. 6 compare relatively well with the UKMO analyses, except in June and July where they are slightly higher than the UKMO average for the month. Analysis of the difference between the POAM III extinction derived PSC occurrence and that from the UKMO analyses, shown in the lower panel of Fig. 6, suggests that the difference in June could be explained by the increased incidence of T_{NAT} threshold crossings caused by the inclusion of gravity waves in the CHAMP observations. However, the much larger differences in other months suggest that the use of a simple T_{NAT} threshold after June is probably not appropriate. This may be explained by recent observations which suggest that the T_{STS} temperature threshold may be a better measure of PSC existence (Pitts et al., 2007). However, this can only explain the reduced PSC incidence later in the year not the enhanced incidence observed in June. Note similar patterns are also observed in 2002.

Poole and Pitts (1994) have examined the relationship between PSC frequency and temperature previously and shown that PSC formation in the southern hemisphere is less likely later in the PSC season than earlier. Other studies, such as Mergenthaler et al. (1997) have suggested that PSC formation late in PSC season in the southern hemisphere is strongly affected by the preceding denitrification and dehydration which fits with the observations displayed in Figs. 4 and 2. Saitoh et al. (2006) also suggests that PSC frequency depends on the degree of denitrification later in the season. Their study also indicates that T_{NAT} is not a good measure of PSC occurrence especially above 20 km in late winter.

Figure 7 displays time-altitude contour plots of the median temperature observed by UKMO analyses and CHAMP RO observations in 2005. The black contour line in both panels of Fig. 7 displays the 195 K contour line from the UKMO analyses for reference purposes. Figure 7 can be used to identify whether the increased T_{NAT} occurrence probability observed in Fig. 6 is associated with temperature perturbations or biases in the temperatures identified in the UKMO analyses compared to the CHAMP RO observations. We remove the affect of gravity wave perturbations on the CHAMP RO observations by using a 4th order polynomial filter. Examination shows that the CHAMP RO observations are slightly cooler than the UKMO analyses in June. In July to August the temperatures are extremely similar and in September and October the temperatures of the UKMO analyses are slightly cooler than the CHAMP observations. Over the entire period the mean bias between the two sets of data is very small (~ -0.08 K). Similar analysis for 2002, 2003 and 2004 shows mean differences of −0.24, 0.2 and 0.47 K, respectively. All four years display cooler CHAMP RO measurements than those from the UKMO analyses and very similar temperatures in July and August (not shown). The similarity of the bias in each year compared to the change in the difference between the estimated PSC occurrence based on temperature information and POAM III observations suggests that the difference can not be solely explained by bias in the UKMO temperatures.

4 Discussion

While temperature biases may explain some of the differences observed between temperature threshold crossing frequencies and the frequency of PSC observed by POAM III extinction measurements further analysis highlights some interesting information. For example, inspection suggests that some features of the data may point to a role for internal gravity wave temperature perturbations. Figure 8 displays a time-longitude contour plot for 2005 of the probability of PSC formation based on POAM III observations. Examination of Fig. 7 shows that an enhanced PSC probability, which relates to the enhancements in June described previously in relation to Fig. 8, occurs around a longitude of 300° E. This longitude corresponds to the position of the Antarctic peninsula which has previously been identified as a "hotspot" for gravity wave activity by Baumgaertner and McDonald (2007) and several other studies. Thus, the expectation that a region of high gravity wave activity might be associated with "enhanced" PSC occurrence is confirmed in this case. It should be noted that MIPAS measurements have identified enhanced PSC occurrence associated with Mountain waves in this area earlier in the same month (Hopfner et al., 2006). This analysis therefore suggests that Mountain waves may play a significant role in enhanced PSC formation.

As previously indicated Fig. 4 shows that during June the number of PSC observed is greater than expected based on the occurrence of regions where the T_{NAT} and T_{STS} temperature thresholds are crossed in some years, most clearly 2002 and 2005 but also for a short period in 2003. A previous study by Saitoh et al. (2006) using ILAS-II observations from 2003 shows a corresponding enhanced PSC frequency compared to that expected based on temperature thresholds. This is a strong validation of the results presented in this study since Saitoh et al. (2006) uses the mean plus five standard deviations from the ILAS-II aerosol extinction data to identify PSC, an extremely conservative threshold.

Figure 9 displays the probability of temperatures below the T_{NAT} temperature threshold against the probability of the threshold crossing being associated with a gravity wave perturbation based on CHAMP RO observations. The second parameter was calculated by identifying all those temperature profiles where the T_{NAT} threshold was crossed and comparing whether the T_{NAT} threshold was crossed if only the mean temperature structure, identified using a 4th order polynomial fit to the CHAMP profile and thereby removing small vertical scale motions. In this way it is possible to determine the proportion of threshold crossings that would only occur if the temperature perturbation is included. Figure 9 suggests that temperature perturbations associated with gravity waves account for approximately 40% of T_{NAT} temperature threshold crossings in June and roughly 15% in other months. This suggests that gravity waves may have a significant impact early in the PSC formation season when the mean temperature is close to the T_{NAT} threshold. This may explain the very clear identification of Mountain waves as the source of PSC detailed in Hopfner et al. (2006). The value for the months other than June compare extremely well with the estimate indicated in Innis and Klekociuk (2006) that gravity wave perturbations influence PSC formation approximately 15% of the time. It should also be noted that Felton et al. (2007) suggests, based on observations from the SOLVE/THESO campaign, that the presence of Type 1a – enhanced PSCs, first identified by Tsias et al. (1999), accounts for about 11% of the PSC observations in the Arctic during the APE-POLECAT campaign.

Similar analysis to that shown in Fig. 9 for the T_{STS} and T_{ICE} temperature thresholds shows relatively similar results; that is an increased frequency of crossing the thresholds associated with gravity wave perturbations. However, the seasonal patterns are shifted towards colder months as might be expected. In addition, no extra threshold crossings associated with T_{STS} and T_{ICE} are observed in June. Given that NAT particles are usually considered to form at temperatures several degrees colder than T_{NAT} (Tabazadeh et al., 2001) or at even lower temperatures (Carslaw et al., 1998) the quantity of PSC observed by POAM III is a little surprising and supports studies such as Voigt et al. (2005) which suggest that there is a mechanism for NAT PSC formation that requires temperatures no lower than a few degrees below T_{NAT}.

It is also worthy of mention that the latitudinal variation for solar occultation satellite observations may mean that some of the patterns could be biased by sampling issues. For example, Pitts et al. (2007) has shown that sampling CALIPSO data at POAM III latitudes moves the maximum PSC occurrence date from early August to September due to the POAM III sampling being at the highest latitude sampled (see Fig. 8). The sampling pattern of POAM III may also bias the relative importance of gravity waves since Wang et al. (2008) indicated that PSCs formed by Mountain waves tend to be localized along the coast of Antarctica and thus we could be overestimating the importance of gravity waves during June and July (see Fig. 8).

5 Conclusions

Examination of Fig. 4 shows that PSC occurrence can be relatively well predicted by the presence of temperatures below either the T_{NAT} or T_{STS} thresholds. This is particularly true if varying water vapour and nitric acid concentrations are taken into account. However, in some years more PSC than might be expected from examination of simple temperature thresholds applied to UKMO analyses are observed in June. The lack of simultaneous nitric acid measurements means that during periods of denitrification the temperature thresholds significantly overestimate PSC occurrence, this is particularly clear in October in several years.

When focusing on the June results examination of the probability of temperatures below the T_{NAT} threshold based on high vertical resolution CHAMP observations show a slightly improved predictive capability compared to the PSC occurrence derived from POAM III extinction data. This may be associated with a warm bias in the UKMO temperature data compared to CHAMP RO measurements. Further analysis of the CHAMP temperature observations suggests that temperature perturbations associated with gravity waves are important in explaining the enhanced PSC incidence observed in June compared to the UKMO analyses. Examination of the longitudinal structure in June 2005 also shows that the enhanced PSC occurrence is close to the Antarctic peninsula a known Mountain wave hotspot. Analysis also suggests that the temperature perturbations produced by gravity waves are most important early in the Antarctic winter, but have a small effect throughout the winter. Based on Fig. 8 temperature perturbations associated with gravity waves contribute to the formation of about 15% of the the T_{NAT} threshold crossings observed, a value which corresponds well to previous studies by Innis and Klekociuk (2006) and Felton et al. (2007). It should be noted that overall the increased incidence of PSC associated with gravity waves seems to

ACPD
9, 3401–3434, 2009

be accounted for by biases in the UKMO analyses. However, studies which focus on ozone depletion in the early period of the Antarctic winter may need to be aware or parameterize for the affect of gravity waves on PSC formation. In the future we aim to complete a more conclusive study by using measurements from CALIPSO and the COSMIC satellites.

Acknowledgements. We are grateful to the GFZ Potsdam and the ISDC for providing the CHAMP data. The POAM III data is kindly provided at http://wvms.nrl.navy.mil/POAM/data/data.html. AJM would like to acknowledge the support provided by the Brian Mason Scientific and Technical Trust. AJM would also like to thank Rebecca Batchelor and Simon Alexander for useful comments on an early version of this work.

References

Alfred, J., Fromm, M., Bevilacqua, R., Nedoluha, G., Strawa, A., Poole, L., and Wickert, J.: Observations and analysis of polar stratospheric clouds detected by POAM III and SAGE III during the SOLVE II/VINTERSOL campaign in the 2002/2003 Northern Hemisphere winter, Atmos. Chem. Phys., 7, 2151–2163, 2007, http://www.atmos-chem-phys.net/7/2151/2007/. 3412, 3414

Baumgaertner, A. J. G. and McDonald, A. J.: A gravity wave climatology for Antarctica compiled from Challenging Minisatellite Payload/Global Positioning System (CHAMP/GPS) radio occultations, J. Geophys. Res.-Atmos., 112, D05103, doi:10.1029/2006JD007504, 2007. 3404, 3418

Carslaw, K. S., Luo, B. P., Clegg, S. L., Peter, T., Brimblecombe, P., and Crutzen, P. J.: Stratospheric Aerosol Growth and Hno3 Gas-Phase Depletion from Coupled Hno3 and Water-Uptake by Liquid Particles, Geophys. Res. Lett., 21, 2479–2482, 1994. 3405, 3411, 3413

Carslaw, K. S., Wirth, M., Tsias, A., Luo, B. P., Dornbrack, A., Leutbecher, M., Volkert, H., Renger, W., Bacmeister, J. T., Reimers, E., and Peter, T. H.: Increased stratospheric ozone depletion due to mountain-induced atmospheric waves, Nature, 391, 675–678, 1998. 3403, 3404, 3414, 3419

Felton, M. A., A., K. T., Omar, A. H., and A., H. C.: Classification of Polar Stratospheric Clouds

Using LIDAR Measurements From the SAGE III Ozone Loss and Validation Experiment, Tech. Rep. ARL-TR-4154, 2007. 3405, 3409, 3419, 3420

Fromm, M., Alfred, J., and Pitts, M.: A unified, long-term, high-latitude stratospheric aerosol and cloud database using SAM II, SAGE II, and POAM II/III data: Algorithm description, database definition, and climatology, J. Geophys. Res.-Atmos., 108(D12), 43666, doi:10.1029/2002JD002772, 2003. 3409, 3410

Fromm, M. D., Lumpe, J. D., Bevilacqua, R. M., Shettle, E. P., Hornstein, J., Massie, S. T., and Fricke, K. H.: Observations of Antarctic polar stratospheric clouds by POAM II: 1994–1996, J. Geophys. Res.-Atmos., 102, 23 659–23 672, 1997. 3410

Hanson, D. and Mauersberger, K.: Laboratory Studies of the Nitric-Acid Trihydrate – Implications for the South Polar Stratosphere, Geophys. Res. Lett., 15, 855–858, 1988. 3404, 3405, 3406, 3411, 3426

Hitchman, M. H., Buker, M. L., Tripoli, G. J., Browell, E. V., Grant, W. B., McGee, T. J., and Burris, J. F.: Nonorographic generation of Arctic polar stratospheric clouds during December 1999, J. Geophys. Res.-Atmos., 108(D5), 8325, doi:10.29/2001JD001034, 2003. 3405, 3413

Hopfner, M., Blumenstock, T., Hase, F., Zimmermann, A., Flentje, H., and Fueglistaler, S.: Mountain polar stratospheric cloud measurements by ground based FTIR solar absorption spectroscopy, Geophys. Res. Lett., 28, 2189–2192, 2001. 3403

Höpfner, M., Larsen, N., Spang, R., Luo, B. P., Ma, J., Svendsen, S. H., Eckermann, S. D., Knudsen, B., Massoli, P., Cairo, F., Stiller, G., v. Clarmann, T., and Fischer, H.: MIPAS detects Antarctic stratospheric belt of NAT PSCs caused by mountain waves, Atmos. Chem. Phys., 6, 1221–1230, 2006, http://www.atmos-chem-phys.net/6/1221/2006/. 3403, 3404, 3418, 3419

Huck, P. E., McDonald, A. J., Bodeker, G. E., and Struthers, H.: Interannual variability in Antarctic ozone depletion controlled by planetary waves and polar temperature, Geophys. Res. Lett., 32, L13819, doi:10.1029/2005GL022943, 2005. 3407

Innis, J. L. and Klekociuk, A. R.: Planetary wave and gravity wave influence on the occurrence of polar stratospheric clouds over Davis Station, Antarctica, seen in lidar and radiosonde observations, J. Geophys. Res.-Atmos., 111, D22102, doi:10.1029/2006JD007629, 2006. 3403, 3404, 3405, 3415, 3419, 3420

Irie, H., Pagan, K. L., Tabazadeh, A., Legg, M. J., and Sugita, T.: Investigation of polar stratospheric cloud solid particle formation mechanisms using ILAS and AVHRR observations in the Arctic, Geophys. Res. Lett., 31, L15107, doi:10.1029/2004GL020246, 2004. 3406

Jakob, C. and Tselioudis, G.: Objective identification of cloud regimes in the Tropical Western Pacific, Geophys. Res. Lett., 30, 2082, doi:10.1029/2003GL018367, 2003. 3408, 3409
Lowe, D. and MacKenzie, A. R.: Polar stratospheric cloud microphysics and chemistry, J. Atmos. Sol.-Terr. Phy., 70, 13–40, 2008. 3403
Lucke, R. L., Korwan, D. R., Bevilacqua, R. M., Hornstein, J. S., Shettle, E. P., Chen, D. T., Daehler, M., Lumpe, J. D., Fromm, M. D., Debrestian, D., Neff, B., Squire, M., Konig-Langlo, G., and Davies, J.: The Polar Ozone and Aerosol Measurement (POAM) III instrument and early validation results, J. Geophys. Res.-Atmos., 104, 18 785–18 799, 1999. 3408
McDonald, A. J. and Hertzog, A.: Comparison of stratospheric measurements made by CHAMP radio occultation and Strateole/Vorcore in situ data, Geophys. Res. Lett., 35, L11805, doi:10.1029/2008GL033338, 2008. 3410
Mergenthaler, J. L., Kumer, J. B., Roche, A. E., and Massie, S. T.: Distribution of Antarctic polar stratospheric clouds as seen by the CLAES experiment, J. Geophys. Res.-Atmos., 102, 19 161–19 170, 1997. 3416
Nedoluha, G. E., Bevilacqua, R. M., Fromm, M. D., Hoppel, K. W., and Allen, D. R.: POAM measurements of PSCs and water vapor in the 2002 Antarctic vortex, Geophys. Res. Lett., 30, 1796, doi:10.1029/2003GL017577, 2003. 3411, 3414
Noel, V., Hertzog, A., Chepfer, H., and Winker, D. M.: Polar stratospheric clouds over Antarctica from the CALIPSO spaceborne lidar, J. Geophys. Res.-Atmos., 113, D02205, doi:10.1029/2007JD008616, 2008. 3404
Pagan, K. L., Tabazadeh, A., Drdla, K., Hervig, M. E., Eckermann, S. D., Browell, E. V., Legg, M. J., and Foschi, P. G.: Observational evidence against mountain-wave generation of ice nuclei as a prerequisite for the formation of three solid nitric acid polar stratospheric clouds observed in the Arctic in early December 1999, J. Geophys. Res.-Atmos., 109, D04312, doi:10.1029/2003JD003846, 2004. 3406, 3413
Parrondo, M. C., Yela, M., Gil, M., von der Gathen, P., and Ochoa, H.: Mid-winter lower stratosphere temperatures in the Antarctic vortex: comparison between observations and ECMWF and NCEP operational models, Atmos. Chem. Phys., 7, 435–441, 2007, http://www.atmos-chem-phys.net/7/435/2007/. 3407
Pawson, S., Kruger, K., Swinbank, R., Bailey, M., and O'Neill, A.: Intercomparison of two stratospheric analyses: Temperature relevant to polar stratospheric cloud formation, J. Geophys. Res., 104, 2041–2050, 1999. 3407
Peter, T.: Microphysics and heterogeneous chemistry of polar stratospheric clouds, Annu. Rev.

ACPD
9, 3401–3434, 2009

Phys. Chem., 48, 785–822, 1997. 3405
Pitts, M. C., Thomason, L. W., Poole, L. R., and Winker, D. M.: Characterization of Polar Stratospheric Clouds with spaceborne lidar: CALIPSO and the 2006 Antarctic season, Atmos. Chem. Phys., 7, 5207–5228, 2007, http://www.atmos-chem-phys.net/7/5207/2007/. 3404, 3413, 3416, 3419
Poole, L. R. and Pitts, M. C.: Polar Stratospheric Cloud Climatology Based on Stratospheric Aerosol Measurement-Ii Observations from 1978 to 1989, J. Geophys. Res.-Atmos., 99, 13 083–13 089, 1994. 3403, 3408, 3416
Saitoh, N., Hayashida, S., Sugita, T., Nakajima, H., Yokota, T., and Sasano, Y.: Variation in PSC Occurrence Observed with ILAS-II over the Antarctic in 2003, SOLA, 2, 72–75, 2006. 3408, 3414, 3416, 3418
Santee, M. L., Lambert, A., Read, W. G., Livesey, N. J., Cofield, R. E., Cuddy, D. T., Daffer, W. H., Drouin, B. J., Froidevaux, L., Fuller, R. A., Jarnot, R. F., Knosp, B. W., Manney, G. L., Perun, V. S., Snyder, W. V., Stek, P. C., Thurstans, R. P., Wagner, P. A., Waters, J. W., Muscari, G., de Zafra, R. L., Dibb, J. E., Fahey, D. W., Popp, P. J., Marcy, T. P., Jucks, K. W., Toon, G. C., Stachnik, R. A., Bernath, P. F., Boone, C. D., Walker, K. A., Urban, J., and Murtagh, D.: Validation of the Aura Microwave Limb Sounder HNO_3 measurements, J. Geophys. Res.-Atmos., 112, D24540, doi:10.1029/2007JD008721, 2007. 3411
Shibata, T., Sato, K., Kobayashi, H., Yabuki, M., and Shiobara, M.: Antarctic polar stratospheric clouds under temperature perturbation by nonorographic inertia gravity waves observed by micropulse lidar at Syowa Station, J. Geophys. Res.-Atmos., 108(D3), 4105, doi:10.1029/2002JD002713, 2003. 3403, 3404
Solomon, S., Garcia, R. R., Rowland, F. S., and Wuebbles, D. J.: On the Depletion of Antarctic Ozone, Nature, 321, 755–758, 1986. 3403
Strawa, A. W., Drdla, K., Fromm, M., Pueschel, R. F., Hoppel, K. W., Browell, E. V., Hamill, P., and Dempsey, D. P.: Discriminating types Ia and Ib polar stratospheric clouds in POAM satellite data, J. Geophys. Res.-Atmos., 107(D20), 8291, doi:10.1029/2001JD000458, 2002. 3409
Svendsen, S. H., Larsen, N., Knudsen, B., Eckermann, S. D., and Browell, E. V.: Influence of mountain waves and NAT nucleation mechanisms on polar stratospheric cloud formation at local and synoptic scales during the 1999-2000 Arctic winter, Atmos. Chem. Phys., 5, 739–753, 2005, http://www.atmos-chem-phys.net/5/739/2005/. 3405, 3413

Tabazadeh, A., Jensen, E. J., Toon, O. B., Drdla, K., and Schoeberl, M. R.: Role of the stratospheric polar freezing belt in denitrification, Science, 291, 2591–2594, 2001. 3414, 3419
Teitelbaum, H., Moustaoui, M., and Fromm, M.: Exploring polar stratospheric cloud and ozone minihole formation: The primary importance of synoptic-scale flow perturbations, J. Geophys. Res.-Atmos., 106, 28 173–28 188, 2001. 3404
Tsias, A., Wirth, M., Carslaw, K. S., Biele, J., Mehrtens, H., Reichardt, J., Wedekind, C., Weiss, V., Renger, W., Neuber, R., von Zahn, U., Stein, B., Santacesaria, V., Stefanutti, L., Fierli, F., Bacmeister, J., and Peter, T.: Aircraft lidar observations of an enhanced type Ia polar stratospheric clouds during APE-POLECAT, J. Geophys. Res.-Atmos., 104, 23 961–23 969, 1999. 3403, 3419
Voigt, C., Schlager, H., Luo, B. P., Drnbrack, A., Roiger, A., Stock, P., Curtius, J., Vssing, H., Borrmann, S., Davies, S., Konopka, P., Schiller, C., Shur, G., and Peter, T.: Nitric Acid Trihydrate (NAT) formation at low NAT supersaturation in Polar Stratospheric Clouds (PSCs), Atmos. Chem. Phys., 5, 1371–1380, 2005, http://www.atmos-chem-phys.net/5/1371/2005/. 3405, 3419
Wang, K. Y. and Lin, S. C.: First continuous GPS soundings of temperature structure over Antarctic winter from FORMOSAT-3/COSMIC constellation, Geophys. Res. Lett., 34, L12805, doi:10.1029/2007GL030159, 2007. 3406, 3407
Wang, Z., Stephens, G., Deshler, T., Trepte, C., Parish, T., Vane, D., Winker, D., Liu, D., and Adhikari, L.: Association of Antarctic polar stratospheric cloud formation on tropospheric cloud systems, Geophys. Res. Lett., 35, L13806, doi:10.1029/2008GL034209, 2008. 3404, 3419
Wickert, J., Schmidt, T., Beyerle, G., Konig, R., and Reigber, C.: The radio occultation experiment aboard CHAMP: Operational data analysis and validation of vertical atmospheric profiles, J. Meteorol. Soc. Jpn., 82, 381–395, 2004. 3410
World Meteorological Organization: Scientific Assessment of Ozone Depletion: 2006, Global Ozone Research and Monitoring Project – Report No. 50, 572 pp., Geneva, Switzerland, 2007. 3406
Wu, D. L. and Jiang, J. H.: MLS observations of atmospheric gravity waves over Antarctica, J. Geophys. Res.-Atmos., 107(D24), 4773, doi:10.1029/2002JD002390, 2002. 3404

ACPD
9, 3401–3434, 2009

Title Page
Abstract | Introduction
Conclusions | References
Tables | Figures
◀| |▶
◀ ▶
Back | Close
Full Screen / Esc
Printer-friendly Version
Interactive Discussion

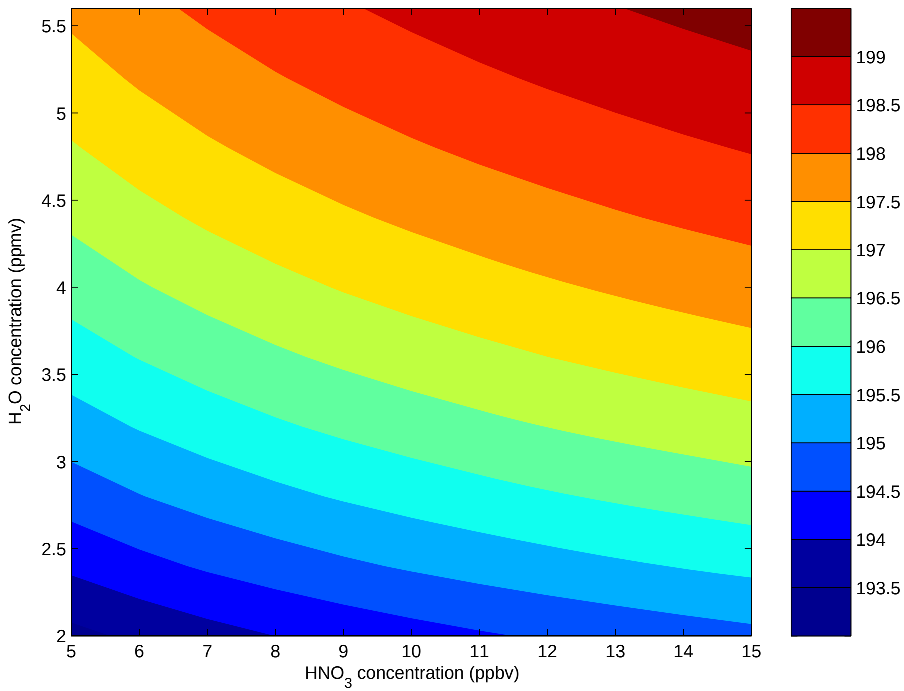

Fig. 1. Contour plot of the NAT PSC formation temperature as a function of nitric acid and water mixing ratios at 18 km. Function based on Hanson and Mauersberger (1988).

ACPD

9, 3401–3434, 2009

PSC occurrence in the Antarctic

A. J. McDonald et al.

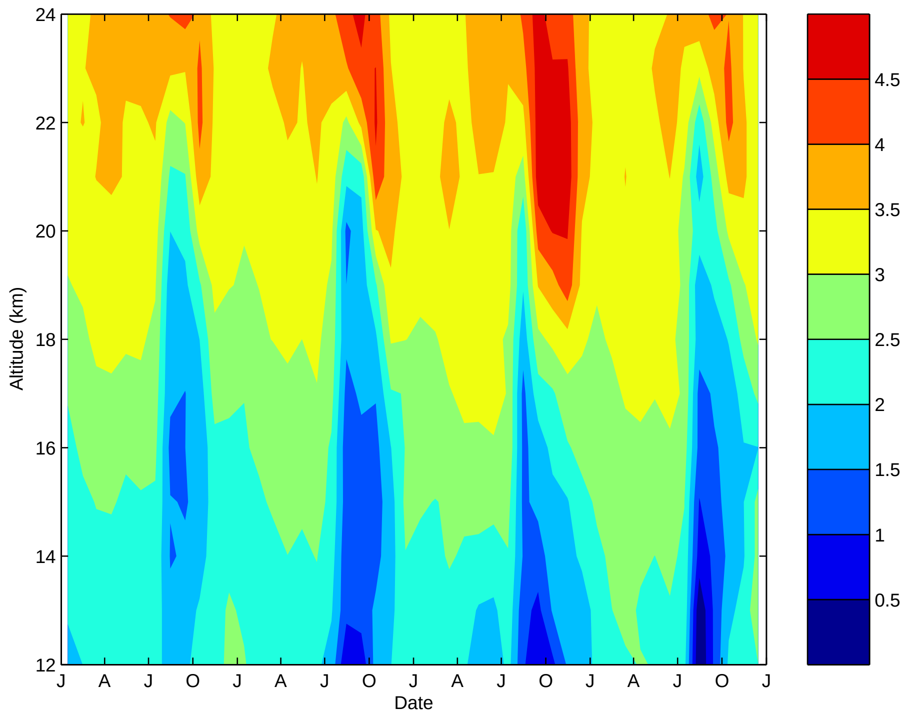

Fig. 2. Time-altitude contour plot of the H_2O mixing ratio derived from POAM III observations for the period January 2002 to December 2005.

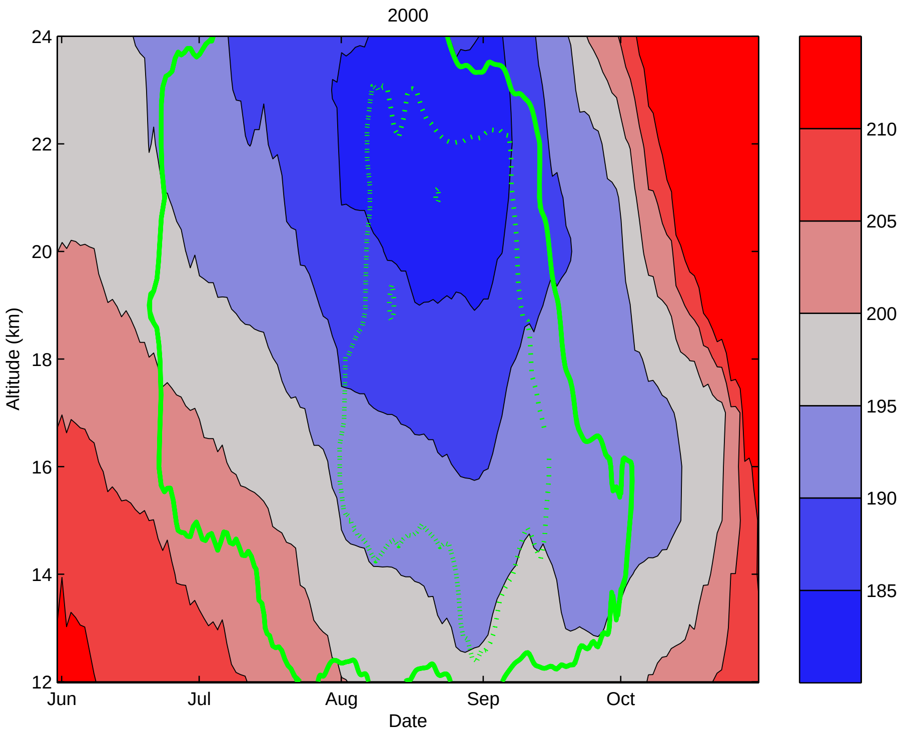

Fig. 3. Time-altitude contour plot of the median UKMO temperature in 2000. The full green line indicates the 25% PSC probability contour and the dotted green line indicates the 75% PSC probability contour, these contours being derived from POAM III extinction measurements. Note that the tick marks on the date axis indicate the first day of the month.

ACPD
9, 3401–3434, 2009

Title Page
Abstract
Introduction
Conclusions
References
Tables
Figures
◀◀
▶▶
◀
▶
Back
Close
Full Screen / Esc
Printer-friendly Version
Interactive Discussion

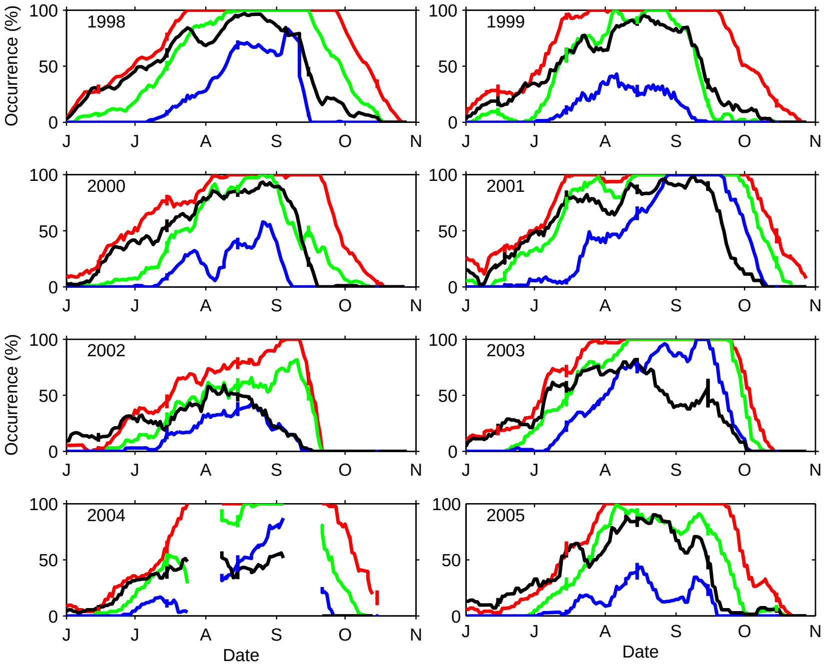

Fig. 4. The probability of temperatures below the T_{NAT} threshold derived from UKMO analyses and using the H_2O variation derived from the POAM III observations and a constant nitric acid mixing ratio of 10 ppbv (red line), the probability of temperatures below the T_{STS} threshold (green line), the probability of temperatures below the T_{ICE} threshold (blue line) and the probability of PSC derived from POAM III extinction measurements (black line) against time of year for the 8 years of POAM III observations. It should be noted that this is the probability at 18km derived over a sliding time window of 10 days. The vertical lines on the fifteenth of each month display the plus and minus one standard deviations for each probability. Note that the tick marks on the date axis indicate the first day of the month.

ACPD

9, 3401–3434, 2009

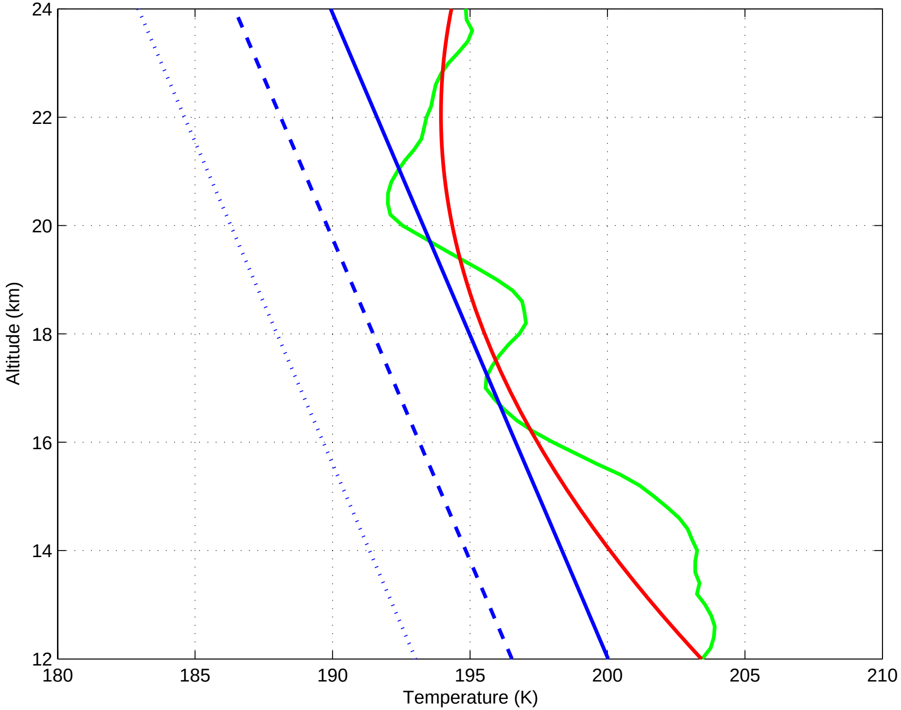

Fig. 5. This diagram shows a CHAMP temperature profile from 2nd June 2006 (green line) and a 4th order polynomial fit to the CHAMP data (red line). The polynomial fit represents the mean temperature observed by CHAMP, the difference between the red and green lines represent temperature perturbations due to gravity waves. The blue full, dashed and dotted lines indicate the values of the T_{NAT}, T_{STS} and T_{ICE} temperature thresholds, respectively.

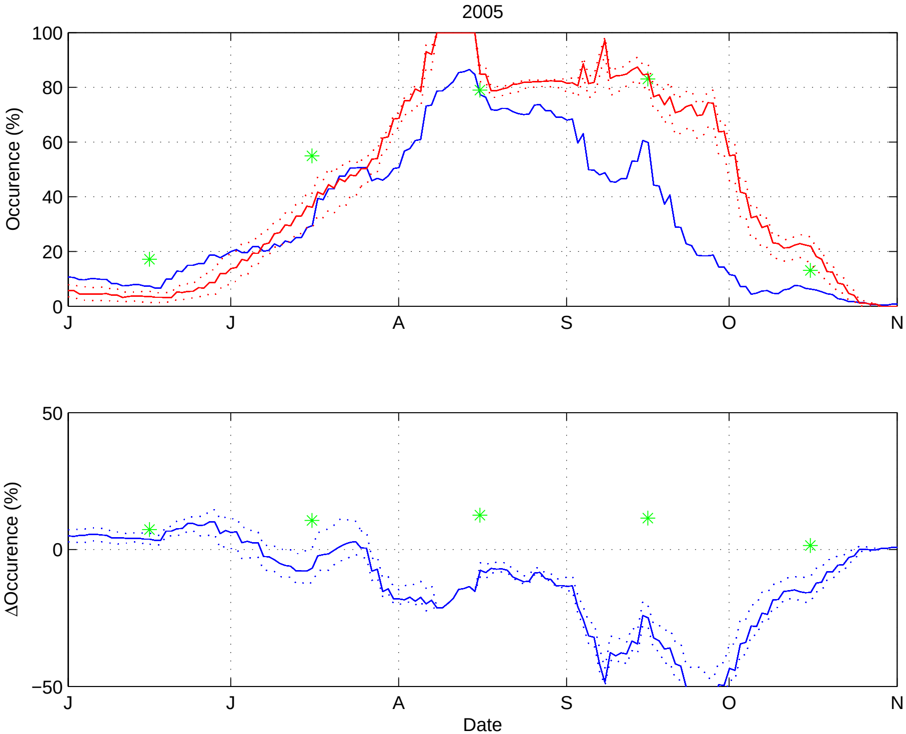

Fig. 6. The top panel displays the probability of the CHAMP temperature measurement being below T_{NAT} (black stars), the probability of the UKMO analyses temperature being below T_{NAT} for HNO_3 mixing ratios of 5 , 10 and 15 ppbv (black lines) and the occurrence of PSC based on POAM III observations between 12 and 24 km for 2005. The lower panel shows the difference between that expected from UKMO analyses and the POAM III observations (grey lines) and the enhanced PSC threshold crossings associated with gravity waves based on CHAMP observations (green stars). The vertical lines on the fifteenth of each month display the plus and minus three standard deviations for each probability.

ACPD
9, 3401–3434, 2009
PSC occurrence in the Antarctic
A. J. McDonald et al.

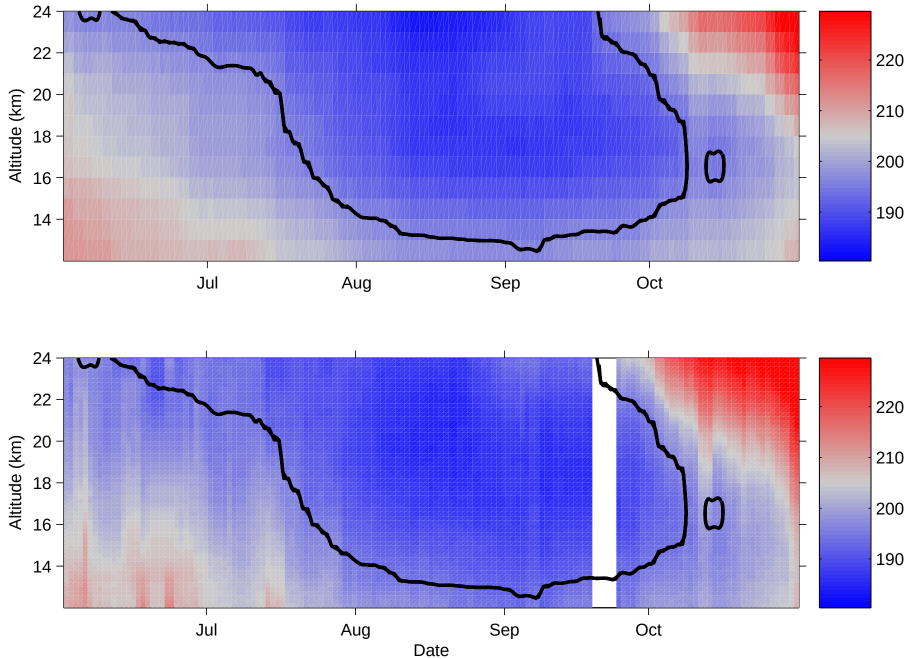

Fig. 7. Time-altitude contour plot of the median temperature derived from UKMO analyses (top panel) and CHAMP radio occultation observations (bottom panel). The black contour line in both panels displays the 195 K contour line from the UKMO analyses. Note that the tick marks on the date axis indicate the first day of the month.

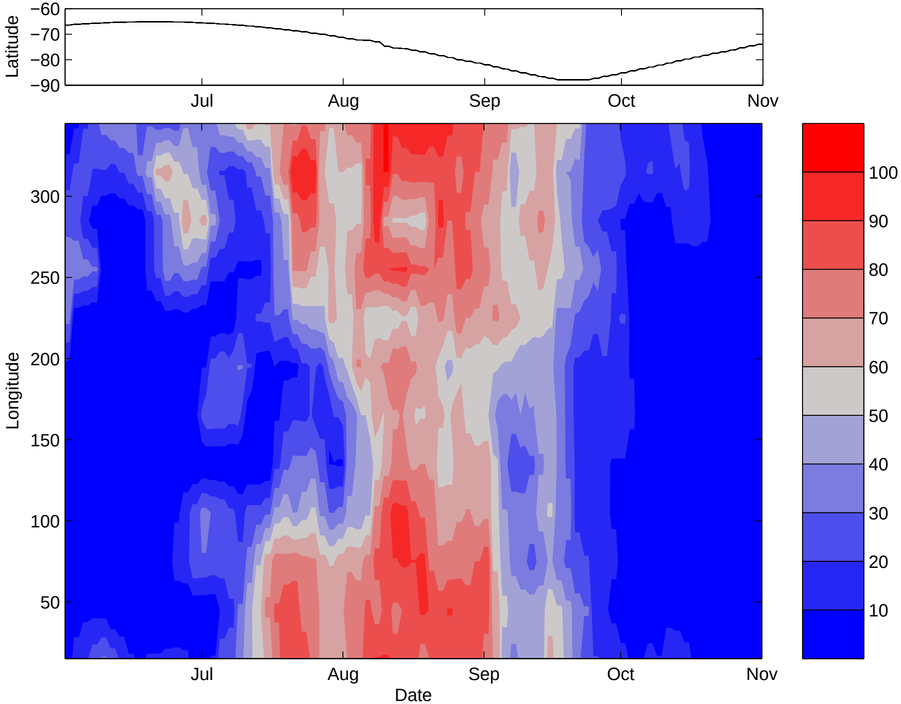

Fig. 8. A plot of the latitude of observations as a function of date (upper panel) and a date-longitude contour plot of the percentage probability of PSC observation derived from POAM III measurements **(b)** for the year 2005. Note that the tick marks on the date axis indicate the first day of the month.

ACPD
9, 3401–3434, 2009

Title Page
Abstract | Introduction
Conclusions | References
Tables | Figures
◀| |▶
◀ ▶
Back | Close
Full Screen / Esc
Printer-friendly Version
Interactive Discussion

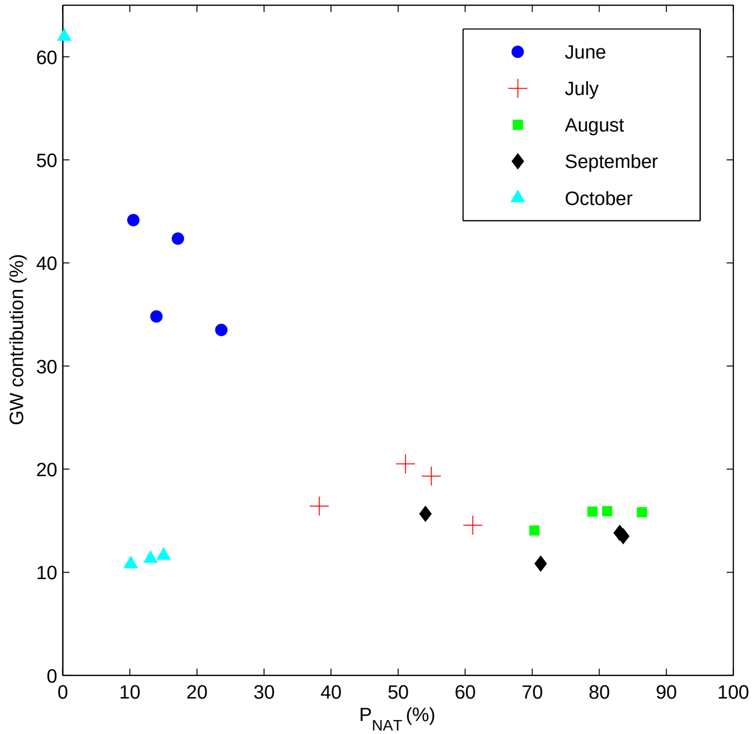

Fig. 9. Probability of observations of temperatures below the NAT nucleation temperature T_{NAT} from CHAMP against the contribution from small-scale wave motions (gravity waves) for different months indicated in the legend.